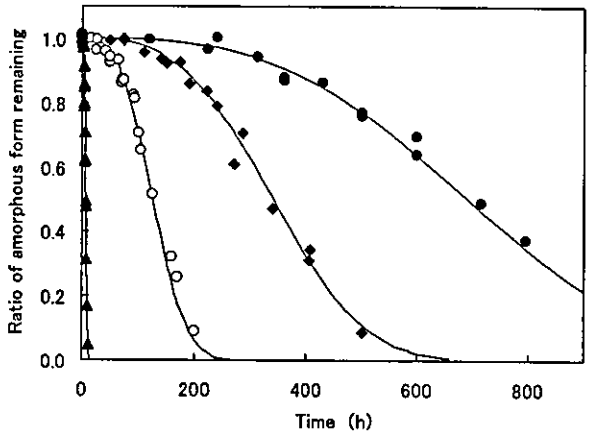

Figure 3. Ratio of the amorphous form remaining in ACTA alone and ACTA/polymer dispersions in the dry state at 40°C. (▲) ACTA; (◆) ACTA/PVP (9:1); (●) ACTA/PAA (9:1); (○) ACTA/PAA (14:1). Solid lines denote the fitting to the Avrami equation.

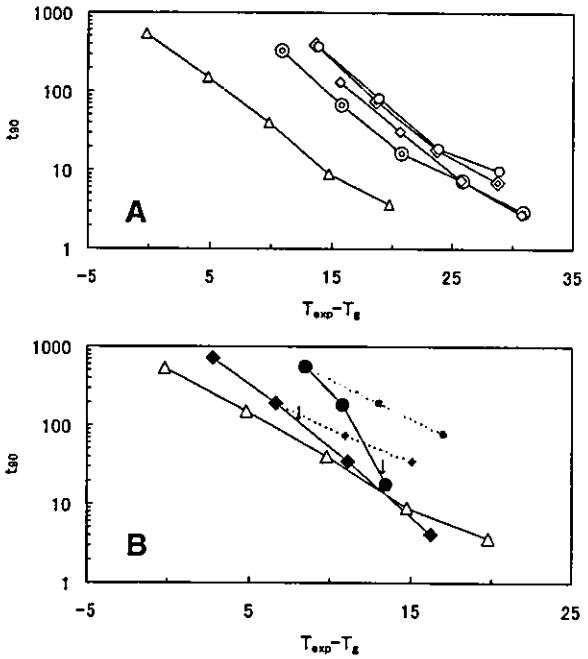

Figure 4. t_{90} obtained in the dry state at various storage temperatures (T_{exp}) (A) and in the moistened conditions (B). (△) dry ACTA; (⊗) dry ACTA/PVP (6:1); (◇) dry ACTA/PVP (9:1); (○) dry ACTA/PAA (9:1); (◎) dry ACTA/PAA (14:1); (◆) ACTA/PVP (9:1) under 11, 33, 57, and 76% RH at 25°C; (●) ACTA/PAA (9:1) under 22, 33, and 57% RH at 25°C; (◈) ACTA/PVP (9:1) under 33% RH at 25, 30, and 35°C; (◉) ACTA/PAA-25 (9:1) under 22% RH at 25, 30, and 35°C. Arrows indicate the ($T_{exp}-T_g$) at which water content corresponds to the saturation of tightly binding sites.

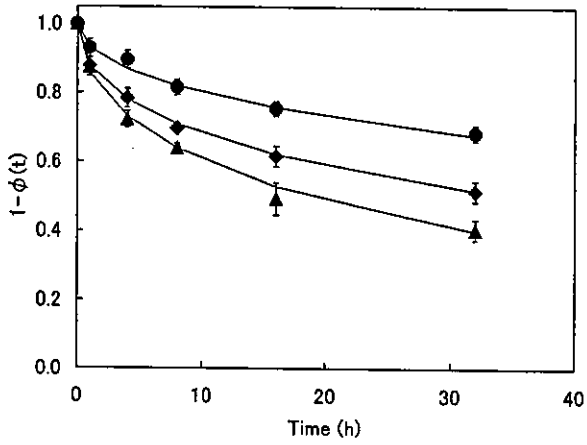

Figure 5. Enthalpy relaxation behavior of amorphous ACTA and ACTA/polymer dispersions. (▲) ACTA; (◆) ACTA/PVP (9:1); (●) ACTA/PAA (9:1). Amorphous ACTA and ACTA/polymer dispersions were stored at 6 and 10°C, respectively. The error bars represent standard deviation ($n > 3$). The lines indicate the fitting to the Kohlrausch-Williams-Watts equation.

where ΔH_t is the enthalpy recovery at time t, and ΔH_∞ is the maximum enthalpy recovery calculated from ΔC_p according to eq. (4):

$$\Delta H_\infty = \Delta C_p \times (T_g - T_a) \quad (4)$$

where T_a is the aging temperature. The T_g and ΔC_p values observed for the sample before storage were used to calculate the ΔH_∞ value. The average relaxation times, τ, calculated according to the Kohlrausch-Williams-Watts equation [eq. (5)][14,15] for ACTA, ACTA/PVP (9:1), and ACTA/PAA (9:1) dispersions were 47 h, 84 h, and 247 h, respectively, with a β value of 0.48.

$$1 - \phi(t) = \exp[(-t/\tau)^\beta] \quad (5)$$

where β is a parameter representing distribution of the relaxation time.

Physical Properties of Absorbed Water in Polymers Determined by DRS

Dielectric relaxation spectra of absorbed water have been described by a sum of two or more relaxation processes.[7–9,16,17] The dielectric relaxation spectra obtained for the lyophilized PVP and PAA with various water contents could be analyzed according to eq. (6) assuming two relaxation processes,

$$\varepsilon^* = \varepsilon_\infty + \Delta\varepsilon_l/(1 + j\omega\tau_l)^{\alpha_l} + \Delta\varepsilon_h/\left(1 + j\omega\tau_h^{\beta_h}\right) \quad (6)$$

where ε^* is the complex permittivity, ε_∞ is the limiting high-frequency permittivity, $\Delta\varepsilon$ is the relaxation strength, τ is the relaxation time, and α and β are parameters representing the distribution of relaxation times. Subscripts l and h represent water with low (-----) and high (——) mobility, respectively. Figure 6 shows the analyzed spectra of the lyophilized PVP and PAA preequilibrated at 76% RH. Tables 2 and 3 show the parameters obtained for PVP and PAA, respectively, at various RH values. The low-frequency process can be attributed to the relaxation of water molecules tightly binding with polymers, because τ_l seemed constant regardless of the water content, and similar to that in references.[7–9,16,17] In contrast, the relaxation peak shown in the high-frequency region is considered to be due to the relaxation of water molecules that weakly interact with polymers, because the τ_h value was smaller than that of bulk water. These parameters obtained for PVP in the high water content region were similar to those reported for a PVP-water solution system.[7] Shinyashiki et al.[9] calculated the number of water molecules corresponding to the saturation of tightly binding sites (n_l) in a collagen-water system from the parameters, $\Delta\varepsilon_h$ and $\Delta\varepsilon_l$, obtained by DRS under the assumption that the ratio of $\Delta\varepsilon_h$ to $\Delta\varepsilon_l$ approximates the ratio of the amount of water with high mobility to that with low mobility. They measured the values of density needed for the calculation. According to this method, the n_l of the lyophilized PVP and PAA was calculated. The density of the samples with various water contents used in the calculation was obtained from the fraction of polymer and its assumed value of density (1.2 g/mL). PVP exhibited an n_l value of 0.5 per monomer unit, which was larger than that obtained for PAA (0.3), indicating that PVP has a greater number of tightly binding sites in the monomer unit.

DISCUSSION

The inhibition effect of a small amount of PVP against crystallization of amorphous sucrose and indomethacin was attributed to the antiplasticization effect of PVP and interaction between PVP and sucrose or indomethacin by Matsumoto and Zografi[2] and Shamblin and Zografi.[3,15] The antiplasticization effect of PVP was confirmed by the finding that the enthalpy relaxation time was prolonged by the presence of PVP. Interaction between PVP and sucrose/indomethacin was confirmed by infrared and Fourier transform-Raman spectroscopy. The authors concluded that formation of indomethacin dimer, which is required for

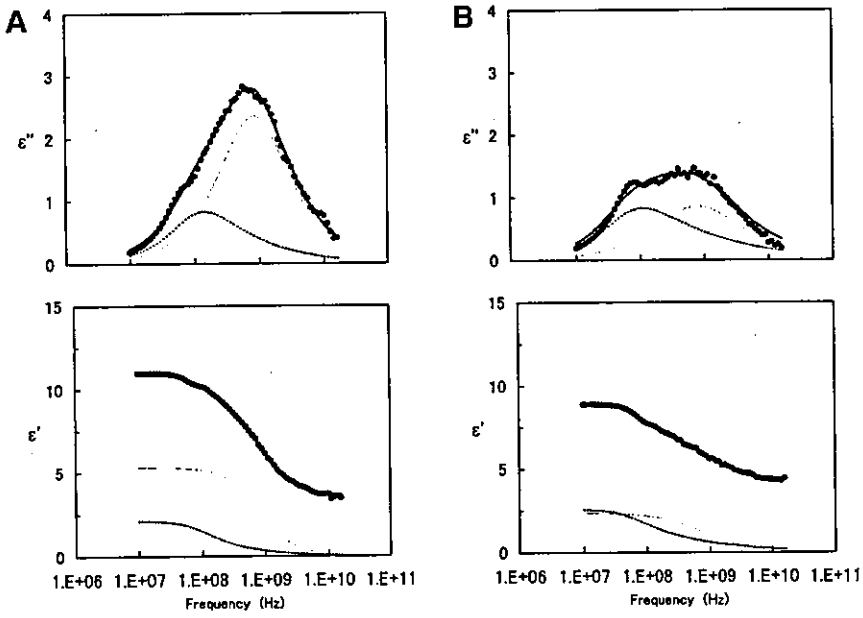

Figure 6. Dielectric absorption ε'' (upper) and dispersion ε' (lower) spectra observed for PVP (A) and PAA (B) at 25°C, 76% RH. (●) experimental data; (-----) relaxation curve for water with low mobility; (——) relaxation curve for water with high mobility; (–) summation of both curves and ε_∞.

nucleation and crystal growth, was inhibited by interaction between PVP and indomethacin. The present study showed that the enthalpy relaxation time of amorphous ACTA was also prolonged by the presence of PVP and PAA (Fig. 5), indicating the decreased molecular mobility of the amorphous ACTA/PVP and ACTA/PAA dispersions in a similar manner as reported for PVP/sucrose and PVP/indomethacin dispersions. Hydrogen bonding between the hydroxyl group and the carbonyl group or amino group of ACTA, which has been reported for ACTA crystals,[12] suggests that the inhibition effect of PVP and PAA against ACTA crystallization can be attributed to the ability of polymers to prevent the association of ACTA molecules in a similar manner as reported for PVP/indomethacin dispersions.[2]

PAA inhibited the crystallization of ACTA more effectively than PVP in the dry state. Nonisothermal crystallization during DSC measurements was not observed in the ACTA/PAA dispersion, but in the ACTA/PVP dispersion with a similar T_g value (Fig. 1c and g). Furthermore, the ACTA/PAA dispersion exhibited a larger t_{90} of isothermal crystallization than the ACTA/PVP dispersion in the temperature range of 45–60°C (Fig. 4A). This stronger stabilizing effect of PAA may be attributed to the larger decrease in molecular mobility. The amorphous dispersions of ACTA/PAA (9:1) and ACTA/PVP (9:1) exhibited about 5 and 2 times longer relaxation time than ACTA alone, respectively, indicating that PAA decreased the molecular mobility of the dispersions more effectively than PVP. The stronger stabilizing effect of PAA may also be due to the stronger interaction between the hydroxyl group of ACTA and the carboxyl group of PAA, rather than the carbonyl group of PVP.

The effect of water to enhance crystallization of amorphous solids is well known.[3–5,18] Shamblin and Zografi[3] and Zhang and Zografi[18] reported that water enhanced the crystallization of sucrose in PVP/sucrose dispersion by plasticizing the amorphous solids and by decreasing PVP–sucrose interaction. The present study also showed that the inhibition effect of PVP against ACTA crystallization was substantially decreased by a small amount of water. The finding that the $(T_{exp}-T_g)$ dependence of t_{90} obtained at various RHs and a constant temperature (25°C) was different from that obtained at a constant RH and various T_{exp}'s (Fig. 4B) suggests that water in ACTA/polymer dispersion inhibits the drug–polymer interaction. PAA exhibited a substantial stabilizing effect in the $(T_{exp}-T_g)$ range smaller than the $(T_{exp}-T_g)$ at which water content corresponded to the saturation of tightly binding sites (indicated by the arrows in Fig. 4B), whereas the stabilizing effect of PVP decreased substantially even in the $(T_{exp}-T_g)$ range smaller than that corresponding to the saturation of tightly binding sites. The difference between PVP and PAA cannot be explained by the difference in the strength of the interaction between water and polymers, because the τ_1 values obtained for PVP and PAA were almost the same (Tables 2 and 3). Therefore, the difference in the strength of drug–polymer interaction may be responsible for the difference in the effect of water on the stabilizing effect of polymers. Further water sorption studies with these solid dispersions seem to be required in a similar manner as those reported for sucrose/PVP and indomethacin/PVP solid dispersions,[3,18,19] in order to discuss the difference in interaction behavior between the ATCA/PVP and ACTA/PAA dispersions.

CONCLUSIONS

The crystallization rate of amorphous ACTA was decreased by co-melting with PAA and PVP. The stabilizing effect of these polymers appeared to be attributed to the decreased average molecular mobility, which was confirmed by the increases in T_g and enthalpy relaxation time. In addition to the decreased molecular mobility, interaction between ACTA and polymers appeared to contribute to the stabilizing effect, as suggested by the finding that the ACTA/PAA dispersion exhibited much slower crystallization than the ACTA/PVP dispersion with a similar T_g value. This stronger effect of PAA may be attributed to the stronger interaction between the hydroxyl group of ACTA and the carboxyl group of PAA, compared with that between the hydroxyl group of ACTA and the carbonyl group of PVP. This explanation is supported by the finding that a small amount of absorbed water decreased the stabilizing effect of PVP. The ability of PAA to decrease the molecular mobility of the amorphous solid dispersion was also larger than that of PVP, as indicated by the longer enthalpy relaxation time.

ACKNOWLEDGMENTS

The authors thank Professor George Zografi, University of Wisconsin-Madison for valuable discussion.

REFERENCES

1. Taylor LS, Zografi G. 1997. Spectroscopic characterization of interactions between PVP and indomethacin in amorphous molecular dispersions. Pharm Res 14:1691–1698.
2. Matsumoto T, Zografi G. 1999. Physical properties of solid molecular dispersions of indomethacin with poly(vinylpyrrolidone) and poly(vinylpyrrolidone-*co*-vinyl-acetate) in relation to indomethacin crystallization. Pharm Res 16:1722–1728.
3. Shamblin SL, Zografi G. 1999. The effects of absorbed water on the properties of amorphous mixtures containing sucrose. Pharm Res 16:1119–1124.
4. Takeuchi H, Yasuji T, Yamamoto H, Kawashima Y. 2000. Temperature- and moisture-induced crystallization of amorphous lactose in composite particles with sodium alginate prepared by spray-drying. Pharm Dev Technol 5:355–363.
5. Forster A, Hempenstall J, Rades T. 2001. Characterization of glass solutions of poorly water-soluble drugs produced by melt extrusion with hydrophilic amorphous polymers. J Pharm Pharmacol 53:303–315.
6. Mashimo S, Kuwabara S, Yagihara S, Higasi K. 1989. The dielectric relaxation of mixtures of water and primary alcohol. J Chem Phys 90: 3292–3294.
7. Shinyashiki N, Asaka N, Mashimo S, Yagihara S. 1990. Dielectric study on dynamics of water in polymer matrix using a frequency range 10^6–10^{10} Hz. J Chem Phys 93:760–764.
8. Shinyashiki N, Matsumura Y, Miura N, Yagihara S, Mashimo S. 1994. Dielectric study of water structure in polymer solution. J Phys Chem 98: 13612–13615.
9. Shinyashiki N, Asaka N, Mashimo S, Yagihara S, Sasaki N. 1990. Microwave dielectric study on hydration of moist collagen. Biopolymers 29:1185–1191.
10. Martino PD, Conflant P, Drache M, Huvenne JP, Guyot-Hermann AM. 1997. Preparation and physical characterization of forms II and III of paracetamol. J Therm Anal 48:447–458.
11. Martino PD, Palmieri GF, Martelli S. 2000. Molecular mobility of the paracetamol amorphous form. Chem Pharm Bull 48:1105–1108.
12. Wang SL, Lin SY, Wei YS. 2002. Transformation of metastable forms of acetaminophen studied by thermal Fourier transform infrared (FT-IR) microspectroscopy. Chem Pharm Bull 50:153–156.
13. Williams ML, Landel RF, Ferry JD. 1955. The temperature dependence of relaxation mechanisms in amorphous polymers and other glass-forming liquids. J Am Chem Soc 77:3701–3707.
14. Hancock BC, Shamblin SL, Zografi G. 1995. Molecular mobility of amorphous pharmaceutical solids below their glass transition temperatures. Pharm Res 12:799–806.
15. Shamblin SL, Zografi G. 1998. Enthalpy relaxation in binary amorphous mixtures containing sucrose. Pharm Res 15:1828–1834.
16. Yoshioka S, Aso Y, Otsuka T, Kojima S. 1995. Water mobility in poly(ethylene glycol)-, poly(vinylpyrrolidone)-, and gelatin-water systems, as indicated by dielectric relaxation time, spin-lattice relaxation time, and water activity. J Pharm Sci 84:1072–1077.
17. Yoshioka S, Aso Y, Kojima S. 1999. The effect of excipients on the molecular mobility of lyophilized formulations, as measured by glass transition temperature and NMR relaxation-based critical mobility temperature. Pharm Res 16:135–140.
18. Zhang J, Zografi G. 2001. Water vapor absorption into amorphous sucrose-poly(vinyl pyrrolidone) and trehalose-poly(vinyl pyrrolidone) mixtures. J Pharm Sci 90:1375–1385.
19. Crowley KJ, Zografi G. 2002. Water vapor absorption into amorphous hydrophobic drug/poly(vinylpyrrolidone) dispersions. J Pharm Sci 90:2150–2165.

Temperature- and Glass Transition Temperature-Dependence of Bimolecular Reaction Rates in Lyophilized Formulations Described by the Adam-Gibbs-Vogel Equation

SUMIE YOSHIOKA, YUKIO ASO, SHIGEO KOJIMA

National Institute of Health Sciences, 1-18-1 Kamiyoga, Setagaya-ku, Tokyo 158-8501, Japan

Received 19 June 2003; revised 24 November 2003; accepted 2 December 2003

Published online 12 February 2004 in Wiley InterScience (www.interscience.wiley.com). DOI 10.1002/jps.20022

ABSTRACT: Bimolecular reaction rates in lyophilized aspirin-sulfadiazine formulations containing poly(vinylpyrrolidone), dextran, and isomalto-oligomers of different molecular weights were determined in the presence of various water contents, and their temperature- and glass transition temperature (T_g)-dependence was compared with that of structural relaxation time (τ calculated according to the Adam-Gibbs-Vogel equation, in order to understand how chemical degradation rates of drugs in lyophilized formulations are affected by molecular mobility. The rate of acetyl transfer in poly(vinylpyrrolidone) K30 and dextran 40k formulations with a constant T_g, observed at various temperatures, exhibited a temperature dependence similar to that of τ at temperatures below T_g. Furthermore, the rates of acetyl transfer and the Maillard reaction in formulations containing α-glucose polymers and oligomers increased, as the T_g of formulations decreased, either associated with decreases in molecular weight of excipient or with increases in water content. The observed T_g dependence was similar to that of τ in the range of T_g higher than the experimental temperature. The results suggest a possibility that bimolecular reaction rate at temperatures below T_g can be predicted from that observed at the T_g on the basis of temperature dependence of structural relaxation time in amorphous systems, if the degradation rate is proportional to the diffusion rate of reacting compounds. © 2004 Wiley-Liss, Inc. and the American Pharmacists Association J Pharm Sci 93:1062–1069, 2004

Keywords: acetyl transfer; lyophilized formulation; glass transition temperature; molecular mobility

INTRODUCTION

The ways in which chemical degradation rates of drugs in lyophilized formulations are affected by molecular mobility largely depend on the degradation mechanism.[1–4] Degradation involving translational or rotational motion of the entire molecule is strongly affected by changes in molecular mobility around the glass transition temperature (T_g), whereas the effect of change in molecular mobility is small for degradation that involves localized motion of specific portions of the molecule. In general, degradation involving bimolecular reactions that require translational motion is largely affected by molecular mobility. Acetyl transfer between aspirin and sulfadiazine in lyophilized formulations containing dextran exhibits a distinct break in temperature dependence, resulting from changes in the translational mobility of the molecules due to glass transition.[5] However, hydrolysis of cephalothin in lyophilized dextran formulations, which is a bimolecular reaction between cephalothin and water, is not significantly affected by changes in molecular mobility, because the diffusion barrier of water molecules is smaller than the activational barrier of hydrolysis.[5]

Correspondence to: Sumie Yoshioka (Telephone: 81-3-3700-8547; Fax: 81-3-3707-6950; E-mail: yoshioka@nihs.go.jp)

Journal of Pharmaceutical Sciences, Vol. 93, 1062–1069 (2004)
© 2004 Wiley-Liss, Inc. and the American Pharmacists Association

The effect of molecular mobility on chemical degradation rates in the amorphous state can be quantitatively evaluated by comparing degradation rates with structural relaxation time τ, which is a useful parameter for indicating molecular mobility. The temperature dependence of τ at temperatures above and below T_g can be described by the Vogel-Tammann-Fulcher (VTF, eq. 1) and Adam-Gibbs-Vogel (AGV, eq. 2) equations, respectively.[6–8]

$$\tau(T) = \tau_0 \exp\left(\frac{DT_0}{T - T_0}\right) \quad (1)$$

$$\tau(T, T_f) = \tau_0 \exp\left(\frac{DT_0}{T - (T/T_f)T_0}\right) \quad (2)$$

where τ_0 is relaxation time at the high temperature limit, and T_f is fictive temperature. D and T_0 are related to the fragility parameter m according to eqs. 3 and 4, respectively.

$$D = 2.303(m_{min})^2/(m - m_{min}) \quad (3)$$

$$T_0 = T_g(1 - m_{min}/m) \quad (4)$$

m_{min} is equal to $\log(\tau_{T_g}/\tau_0)$, where τ_{T_g} is relaxation time at T_g. Comparison of τ and degradation rates has been reported only for chemical degradation of amorphous quinapril hydrochloride[9] and crystallization of amorphous nifedipine.[10] Further quantitative studies with other amorphous systems are required in order to improve our general understanding of the ways in which chemical degradation rates are affected by molecular mobility.

This article describes the relationship between the temperature dependence of structural relaxation time and that of bimolecular reaction rates in lyophilized aspirin-sulfadiazine formulations containing poly(vinylpyrrolidone) (PVP), dextran, and isomalto-oligomers. The T_g of these formulations was controlled by changing the molecular weights of excipient and water contents. Acetyl transfer reaction between aspirin and sulfadiazine, as well as the Maillard reaction between sulfadiazine and the terminal α-glucose unit of oligomers were chosen as bimolecular reaction models.

EXPERIMENTAL

Materials

Dextran 40k, dextran 10k, PVP K90, and sulfadiazine were purchased from Sigma Chemical Co. (St. Louis, MO). PVP K30, isomalto-oligomer (090-03485), aspirin (015-10262), salicylic acid (199-00142), and 4-hydroxybenzoic acid (084-04102) were provided by Wako Pure Chemical Industries Ltd. (Osaka, Japan). Isomalto-oligomer was dialyzed against distilled water using a membrane with a pore size of 2000 molecular weight cutoff (Spectrum Laboratories, Inc., Laguna Hills, CA), frozen by immersion in liquid nitrogen, and then dried in a vacuum of <5 Pa for 23.5 h in a lyophilizer (Freezevac C-1; Tozai Tsusho Co., Tokyo, Japan). Shelf temperature was between −35° and −30°C for the first 1 h, 20°C for the subsequent 19 h, and 30°C for the last 3.5 h. Isomalto-oligomer as received is hereafter referred to as isomalto-oligomer A, whereas that after dialysis and freeze-drying is isomalto-oligomer B. Freeze-drying of isomalto-oligomer A and B yielded cakes with T_g values of 100° and 152°C, respectively.

Preparation of Lyophilized Formulations

A 19.5-g portion of aspirin solution (0.0924% w/w) was added to 20.5 g of sulfadiazine and PVP K30 solution [5 mg of sulfadiazine and 250 mg of PVP K30 (or PVP K90) in 19.5 g of distilled water] to give a final ratio of sulfadiazine/aspirin/PVP K30 (or PVP K90) of 1:3.6:50 w/w. The molecular ratio of sulfadiazine to aspirin was 1:5. Three hundred microliters of these solutions was frozen in polypropylene sample tubes (10-mm diameter) by immersion in liquid nitrogen for 10 min, then dried in a lyophilizer as described above. The solutions before freeze-drying were prepared under ice-cooled conditions to inhibit the hydrolysis of aspirin.

Lyophilized formulations containing dextran 40k, dextran 10k, isomalto-oligomer A, and isomalto-oligomer B were prepared from a sulfadiazine-aspirin-excipient solution (1:3.6:200 w/w). A larger ratio of excipient than that for PVP series formulations was used in order to decrease the reaction rate that is larger than that in PVP series formulations at the same ratio.

Lyophilized formulations with various water contents were obtained by storing at 15°C for 24 h in a desiccator with a saturated solution of LiCl H_2O [12% relative humidity (RH)], potassium acetate (23% RH), $MgCl_2$ $6H_2O$ (33% RH), K_2CO_3 $2H_2O$ (43% RH), $Ca(NO_3)_2$ $4H_2O$ (55% RH), NaBr $2H_2O$ (60% RH), or NaCl (75% RH). Obtained formulations showed the T_g values listed in Table 1, depending on the humidity conditions.

Table 1. T_g of Lyophilized Formulations with Water Contents Adjusted at Various Humidities (°C)

Relative humidity (%)	12	23	33	43	55	60	75
Isomalto-olygomer A	70	50	39	31	6	—	—
Isomalto-olygomer B	83	72	58	44	37	—	—
Dextran 10k	—	98	79	68	45	44	—
Dextran 40k	—	—	89	72	57	50	—
PVP K30	112	85	66	58	45	34	9
PVP K90	—	81	72	58	41	41	7

—, Not determined.

Determination of Degradation Rate

Lyophilized sulfadiazine-aspirin-PVP K30 formulations with T_g values of 112°C and 58°C were stored at temperatures ranging from 20° to 60°C (±0.1°C) after capped tightly with a screw-cap in order to prevent water elimination. The samples were removed at appropriate intervals to determine the amount of remaining sulfadiazine and aspirin.

Samples were dissolved in 1 mL of 50 mM phosphate buffer (pH 2.5), and 0.7 mL of methanol containing 4-hydroxybenzoic acid as an internal standard was added in the solution. The solution was injected into an high-performance liquid chromatography system consisting of a Shimadzu LC-10AD VP pump (Kyoto, Japan), a Shimadzu variable-wavelength UV detector (SDD-M10A), and a Shimadzu CLASS-VP data system. A Tosoh AS-8010 autoinjector (Tokyo, Japan) delivered 20-μL samples. The sulfadiazine, aspirin, salicylic acid, and acetyl sulfadiazine were separated on a reversed-phase column (Inertsil ODS-3, 4.6 mm × 150 mm; GL Science Inc., Tokyo, Japan) maintained at 35°C. The detection wavelength was 200 nm. The mobile phase was a mixture of 50 mM phosphate buffer (pH 2.5) and methanol (3:2).

As previously reported,[5] the rate constant of acetyl transfer (k_T) and the pseudo-rate constant of hydrolysis ($k_{H,pseudo}$) were determined by curve-fitting of the amount of remaining sulfadiazine [SD] and aspirin [ASA] to the following equations (only the initial data points representing <10% reaction were used for the fitting to minimize the effects of salicylic acid and acetic acid formation).

$$d[SD]/dt = -k_T[SD][ASA]$$
$$d[ASA]/dt = -k_T[SD][ASA] - k_{H,pseudo}[ASA]$$

The time required for 10% acetyl transfer (t_{90}) was calculated from the obtained k_T value.

Lyophilized sulfadiazine-aspirin formulations containing dextran 10k and 40k, isomalto-oligomer A and B, and PVP K30 and K90 with various T_g values were stored at 60°C. The samples were removed at appropriate intervals to determine the amount of remaining sulfadiazine by using the high-performance liquid chromatography system described above. Apparent first-order rate constant for decreases in the amount of sulfadiazine was determined by curve-fitting to calculate time required for 10% degradation (t_{90}).

Determination of T_g by Differential Scanning Calorimetry

Lyophilized formulations with various water contents adjusted by storing at 15°C under various humidity conditions were put in a hermetic pan. Thermograms were obtained in the temperature range from 40°C lower than the T_g to 40°C higher than the T_g at a scan rate of 20°C/min by differential scanning calorimetry (2920; TA Instruments, New Castle, DE). Temperature calibration was performed using indium.

RESULTS

Effect of Temperature on t_{90} for Acetyl Transfer in Lyophilized Formulation with a Constant T_g

Sulfadiazine and aspirin underwent acetyl transfer in the lyophilized formulation containing PVP K30 in a similar manner as reported for lyophilized formulations containing dextran and methylcellulose.[5] Figure 1 shows the temperature dependence of t_{90} for acetyl transfer calculated from k_T values observed for PVP K30 formulations with T_g values of 112° and 58°C. A linear temperature dependence of t_{90} was observed at

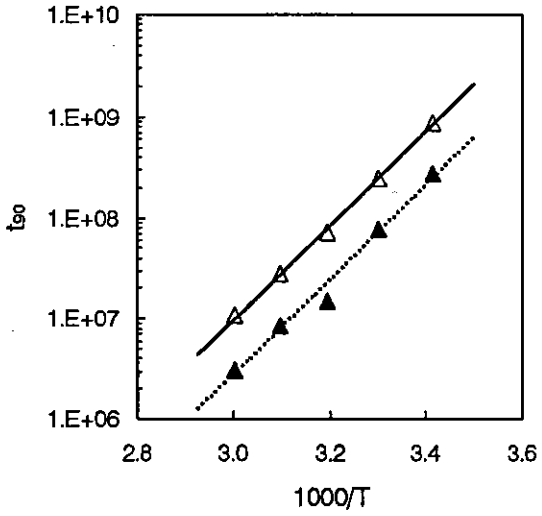

Figure 1. Temperature dependence of t_{90} for acetyl transfer in lyophilized PVP K30 formulations with constant T_g values of 58°C (▲) and 112°C (△).

temperatures substantially lower than the T_g (20–60°C for T_g of 112°C), but there seemed to be a small deviation from the linear line around a temperature approximately 20°C lower than the T_g (35°C for T_g of 58°C).

Effect of Molecular Weight of Excipient and Water Content on t_{90} for Acetyl Transfer and the Maillard Reaction in Lyophilized Formulation

Sulfadiazine underwent only acetyl transfer in the lyophilized sulfadiazine-aspirin formulations containing PVP and dextran, whereas in the lyophilized formulations containing isomalto-oligomers A and B, it underwent the Maillard reaction with the terminal α-glucose unit of oligomer chain in addition to acetyl-transfer reaction with aspirin. Initial decreases in sulfadiazine observed during storage of these formulations were describable with first-order kinetics. The time courses of degradation in isomalto-oligomer B formulation are shown as examples in Figure 2. The apparent first-order rate constant determined from the initial slope corresponded to the rate constant of acetyl transfer for the PVP K90, K30, dextran 40k, and 10k formulations, whereas it corresponded to the overall rate constant including acetyl transfer and the Maillard reactions for the isomalto-oligomer A and B formulations.

Figure 3 shows the t_{90} calculated from the apparent first-order rate constant observed at a

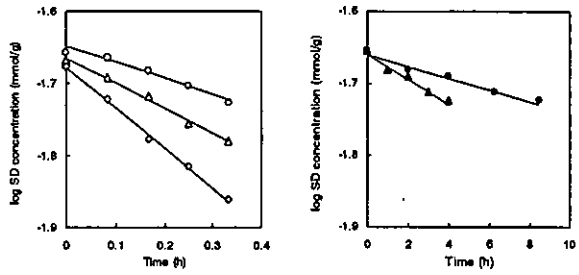

Figure 2. Decrease in the amount of sulfadiazine remaining at 60°C in lyophilized isomalto-oligomer B formulation with T_g values of 83°C (●), 72°C (▲), 59°C (○), 44°C (△), and 37°C (◇).

constant temperature of 60°C in the formulations containing various molecular weights of excipient, plotted against the humidity at which the water content of formulations was adjusted. Significant differences in t_{90} between different molecular weights of excipients were not observed for the PVP series (PVP K30 and K90) formulations, but for the α-glucose series (isomalto-oligomers A and B, and dextrans 10k and 40k) formulations. The t_{90} of the latter formulations was decreased by decreases in the molecular weight of excipient and by increases in humidity (i.e., increases in water content). A rapid change in t_{90} was observed at a lower humidity, as the molecular weight of excipient decreased. Figure 4 shows the t_{90} plotted

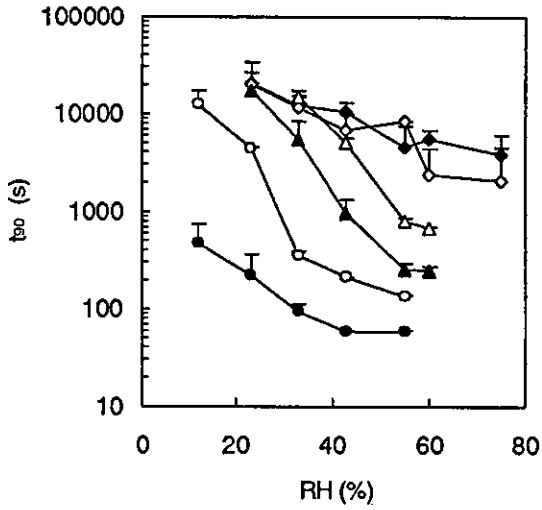

Figure 3. Effect of water content (humidity at which water content was adjusted) on the t_{90} observed at 60°C with lyophilized isomalto-oligomer A (●) and B (○), dextran 10k (▲) and 40k (△), and PVP 30 (◇) and PVP 90 (◆) formulations. SD ($n = 3$).

(eq. 1). The τ value calculated using an m value of 70 according to the VTF equation is just an approximation, because it depended largely on the m value used for the calculation. The temperature dependence of t_{90} for acetyl transfer in these formulations containing PVP K30 and dextran 40k was similar to that of τ calculated based on the AGV equation at temperatures below T_g, although t_{90} values at temperatures far from T_g tended to diverge from the line.

The similarity of temperature dependence between t_{90} and τ at temperatures below T_g suggests that t_{90} for acetyl transfer is related to the molecular mobility of lyophilized formulations. In other words, the rate of acetyl transfer is suggested to be proportional to the diffusion rates of the molecules, as reported for the chemical degradation of quinapril hydrochloride.[9]

As reported previously,[5] the temperature dependence of the acetyl-transfer rate in the lyophilized dextran 40k formulation exhibited a break around a temperature approximately 15°C lower than the T_g, namely T_{mc} at which glass transition began to be detected by nuclear magnetic resonance relaxation measurements.[13] This break is inconspicuous in Figure 5, in which the y-axis is reduced. Similarly, a small divergence from linearity observed in the temperature dependence of t_{90} for acetyl transfer in the PVP K30 formulation with a T_g of 58°C (Fig. 1) becomes inconspicuous in Figure 5.

Dependence of t_{90} for Acetyl Transfer and the Maillard Reaction on the T_g Controlled by Changing the Molecular Weight of Excipient and Water Content

The t_{90} for the α-glucose series formulations tended to decrease as the molecular weight of excipient decreased, when compared at a same value of $(T - T_g)$ (Fig. 4). These differences in t_{90} between different molecular weights can be explained by the Maillard reaction, which occurred along with acetyl transfer in α-glucose series formulations. Increases in the number of the reacting compound for the Maillard reaction (i.e., terminal α-glucose unit) resulted in the decreases in t_{90}. Both acetyl transfer and the Maillard reaction are expected to be molecular mobility-controlled intermolecular reactions. The t_{90} of each of the α-glucose series formulations exhibited a rapid decrease when T_g approached to the experimental temperature in association with increases in water content (Fig. 4).

To compare the t_{90} versus T_g relationship between formulations containing different molecular weights of excipients (i.e., different numbers of terminal α-glucose), the t_{90} for sulfadiazine degradation in the α-glucose series formulations was scaled to the t_{90} value at a point at which T_g is equivalent to the experimental temperature, and is plotted against the T_g value scaled to the experimental temperature in Figure 6. Plots for the PVP series formulations are also included in Figure 6. Figure 6 also shows the T_g dependence of τ calculated based on the AGV equation (eq. 2) by assuming that $\xi = 1$, $T_f = T_g$, and $m = 70$.

The t_{90} for sulfadiazine degradation in the α-glucose series formulations with different T_g values depending on the molecular weight and water content exhibited a similar pattern of T_g dependence to that of τ calculated based on the AGV equation in the range of T_g higher than the experimental temperature, although larger variations were observed compared with Figure 5. This finding indicates that molecular mobility is one of the primary factors that determine the degradation rate. Increases in water content can possibly affect the degradation rate not only by varying the T_g of formulations, but also by acting as a reacting compound. However, it has been reported that water is involved in the rate-determining process for neither acetyl-transfer reaction[14] nor the Maillard reaction.[15]

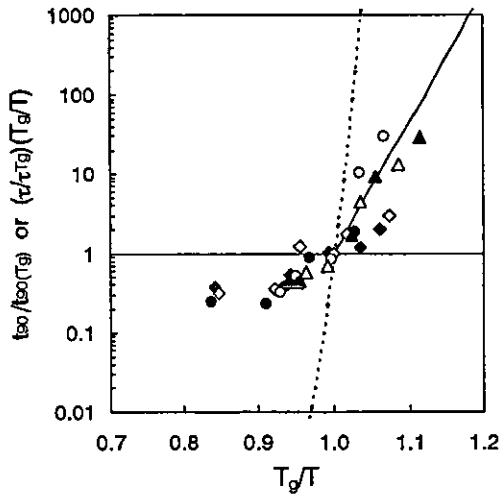

Figure 6. Comparison of the T_g dependence of t_{90} observed at a constant temperature of 60°C in isomaltooligomer A (●) and B (○), dextran 10k (▲) and 40k (△), and PVP 30 (◇) and PVP 90 (◆) formulations with that for structural relaxation time τ calculated according to the AGV equation (solid line) and VTF equation (broken line).

The t_{90} for sulfadiazine degradation in the PVP series formulations was much larger than that in the α-glucose series formulations (Fig. 4). This difference in t_{90} may be attributed to the difference in the type and extent of interaction between the reacting compounds and excipient. The finding that the t_{90} for sulfadiazine degradation in the PVP series formulations diverged from the τ calculated based on the AGV equation (Fig. 6) also suggests that the effect of PVP on the reaction rate is different from that of α-glucose series excipients. This may be explained by assuming that the mobility of reacting compounds in the PVP formulations becomes different from that of the whole formulation determined by τ, when formulations have higher T_g values that resulted from lower water contents. This explanation is supported by the finding that the temperature dependence of t_{90} observed for the PVP formulation with a constant water content tended to diverge from the line at temperatures far from T_g (Fig. 5).

Temperature Dependence of t_{90} in the Range in Which T_g Is Lower Than Experimental Temperature

In the range in which T_g is lower than the experimental temperature, t_{90} exhibited a temperature dependence different from that of τ calculated based on the VTF equation. This is the case for both t_{90} determined at various temperatures for formulations with a constant T_g (Fig. 5) and that determined at a constant temperature for formulations with various T_g values depending on the molecular weight of excipient and water content (Fig. 6). Although the τ value calculated by the VTF equation is just an approximation, the slope for t_{90} can be considered to be much smaller than that for τ. These findings suggest that the acetyl-transfer rate in the range in which T_g is lower than the experimental temperature is not controlled by molecular mobility, but by activational barrier of the reaction. In other words, the diffusion barrier of the molecules is smaller than the activational barrier of the reaction.

CONCLUSIONS

The rate of acetyl transfer, a bimolecular reaction, in lyophilized aspirin-sulfadiazine formulations containing PVP K30 and dextran 40k with a constant T_g exhibited a temperature dependence similar to that of τ described by the AGV equation at temperatures below T_g. Furthermore, the rates of acetyl transfer and the Maillard reaction in the α-glucose series formulations increased with decreases in the T_g of formulations, either associated with decreases in molecular weight of excipient or with increases in water content, and exhibited a similar T_g dependence to that of τ calculated based on the AGV equation in the range of T_g higher than the experimental temperature.

The data obtained using the present model lyophilized formulations suggest a possibility that the rates of bimolecular reactions at temperatures below T_g can be predicted from that determined at T_g on the basis of temperature dependence of structural relaxation time in amorphous systems, if the degradation rate is proportional to the diffusion rate of reacting compounds.

REFERENCES

1. Duddu SP, Weller K. 1996. Importance of glass transition temperature in accelerated stability testing of amorphous solids: Case study using a lyophilized aspirin formulation. J Pharm Sci 85: 345–347.
2. Streefland L, Auffret AD, Franks F. 1998. Bond cleavage reactions in solid aqueous carbohydrate solutions. Pharm Res 15:843–849.
3. Lai MC, Hageman MJ, Schowen RL, Borchardt RT, Topp EM. 1999. Chemical stability of peptides in polymers. II. Discriminating between solvent and plasticizing effects of water on peptide deamidation in poly(vinylpyrrolidone). J Pharm Sci 88:1081–1089.
4. Li J, Guo Y, Zografi G. 2002. The solid-state stability of amorphous quinapril in the presence of β-cyclodextrins. J Pharm Sci 91:229–243.
5. Yoshioka S, Aso Y, Kojima S. 2000. Temperature dependence of bimolecular reactions associated with molecular mobility in lyophilized formulations. Pharm Res 17:925–929.
6. Andronis V, Zografi G. 1998. The molecular mobility of supercooled amorphous indomethacin as a function of temperature and relative humidity. Pharm Res 15:835–842.
7. Tong P, Zografi G. 1999. Solid-state characteristics of amorphous sodium indomethacin relative to its free acid. Pharm Res 16:1186–1192.
8. Shamblin SL, Tang X, Chang L, Hancock BC, Pikal MJ. 1999. Characterization of the time scales of molecular motion in pharmaceutically important glasses. J Phys Chem 103:4113–4121.
9. Guo Y, Byrn SR, Zografi G. 2000. Physical characteristics and chemical degradation of amorphous quinapril hydrochloride. J Pharm Sci 89: 128–143.

10. Aso Y, Yoshioka S, Kojima S. 2001. Explanation of the crystallization rate of amorphous nifedipine and phenobarbital from their molecular mobility as measured by 13C nuclear magnetic resonance relaxation time and the relaxation time obtained from the heating rate dependence of the glass transition temperature. J Pharm Sci 90:798–806.
11. Crowley KJ, Zografi G. 2002. The use of thermal methods for predicting glass-former fragility. Thermochim Acta 380:79–93.
12. Boehmer R, Ngai KL, Angell CA, Plazek DJ. 1993. Nonexponential relaxations in strong and fragile glass formers. J Chem Phys 99:4201–4209.
13. Yoshioka S, Aso Y, Kojima S. 1999. The effect of excipients on the molecular mobility of lyophilized formulations, as measured by glass transition temperature and NMR relaxation-based critical mobility temperature. Pharm Res 16:135–140.
14. Liu L, Parrott EL. 1991. Solid-state reaction between sulfadiazine and acetylsalicylic acid. J Pharm Sci 80:564–566.
15. Craig ID, Parker R, Rigby NM, Cairns P, Ring SG. 2002. Maillard reaction kinetics in model preservation systems in the vicinity of the glass transition: Experiment and theory. J Agric Food Chem 49: 4706–4712.

Molecular Mobility-Based Estimation of the Crystallization Rates of Amorphous Nifedipine and Phenobarbital in Poly(vinylpyrrolidone) Solid Dispersions

YUKIO ASO, SUMIE YOSHIOKA, SHIGEO KOJIMA

National Institute of Health Sciences, 1-18-1, Kamiyoga, Setagaya-ku, Tokyo 158-8501, Japan

Received 13 March 2003; revised 22 July 2003; accepted 29 July 2003

Published online 25 November 2003 in Wiley InterScience (www.interscience.wiley.com). DOI 10.1002/jps.10526

ABSTRACT: The overall crystallization rates and mean relaxation times of amorphous nifedipine and phenobarbital in the presence of poly(vinylpyrrolidone) (PVP) were determined at various temperatures to gain further insight into the effect of molecular mobility on the crystallization rates of amorphous drugs and the possibility of predicting stability from their molecular mobility. Nifedipine–PVP (9:1 w/w) and phenobarbital–PVP (95:5 w/w) solid dispersions were prepared by melting and rapidly cooling mixtures of each drug and PVP. The amount of amorphous nifedipine remaining in the solid dispersion was calculated from the heat of crystallization,which was obtained by differential scanning calorimetry. The amount of amorphous phenobarbital remaining in the solid dispersion was estimated from the change in the heat capacity at its glass transition temperature (T_g). The time required for the amount of amorphous drug remaining to fall to 90% (t_{90}) was calculated from the profile of time versus the amount of amorphous drug remaining. The t_{90} values for the solid dispersions studied were 100–1000 times longer than those of pure amorphous drugs when compared at the same temperature. Enthalpy relaxation of the amorphous drugs in the solid dispersions was reduced compared with that in the pure amorphous drugs, indicating that the molecular mobility of the amorphous drugs is reduced in the presence of PVP. The temperature dependence of mean relaxation time (τ) for the nifedipine–PVP solid dispersion was calculated using the Adam–Gibbs–Vogel equation. Parameters D and T_0 in this equation were estimated from the heating rate dependence of T_g. Similar temperature dependence was observed for t_{90} and τ values of the solid dispersion, indicating that the information on the temperature dependence of the molecular mobility, along with the crystallization data obtained at around the T_g, are useful for estimating the t_{90} of overall crystallization at temperatures below T_g in the presence of excipients. © 2004 Wiley-Liss, Inc. and the American Pharmacists Association J Pharm Sci 93:384–391, 2004

Keywords: crystallization; amorphous; stability; solid dispersion; relaxation time

INTRODUCTION

To improve their dissolution rates and bioavailability, poorly soluble drugs are utilized in the amorphous form. However, instability during storage, as evidenced by crystallization, is an issue of concern with amorphous drugs, and prediction of their stability at room temperature is a matter of great interest. Predicting the stability of amorphous drugs at room temperature from data obtained at higher temperatures is generally considered to be difficult because the temperature dependence of the degradation rate usually differs above and below their glass transition temperatures (T_g). However, because the temperature dependence of the degradation rate has been reported to be similar to that of the molecular mobility for

Correspondence to: Yukio Aso (Telephone: 81-3-3700-8547; Fax: 81-3-3707-6950; E-mail: aso@nihs.go.jp)

Journal of Pharmaceutical Sciences, Vol. 93, 384–391 (2004)
© 2004 Wiley-Liss, Inc. and the American Pharmacists Association

some amorphous drugs,[1,2] it may be possible to predict their stability based on the temperature dependence of the molecular mobility when the stability is governed by molecular mobility.

The crystallization rate, k, of an amorphous solid at temperature T depends on the rate of molecular diffusion across the nuclear–amorphous matrix interface [$D(T)$] and the nucleation free energy term [$f(T)$], according to eq. 1.[3–6]

$$k \propto D(T)f(T) \quad (1)$$

In a previous paper,[7] we reported that the temperature dependence of the overall crystallization rates of pure amorphous nifedipine and phenobarbital is similar to that of the mean relaxation time (τ) calculated according to the Adam–Gibbs–Vogel (AGV) equation (eq. 2),[8] which is a measure of molecular mobility.

$$\tau = \tau_0 \exp\left\{\frac{DT_0}{T(1 - T_0/T_f)}\right\} \quad (2)$$

where D and T_0 are the Vogel–Tammann–Fulcher (VTF) equation parameters, and T_f is the fictive temperature. When $T > T_g$, $T_f = T$ and eq. 2 is identical to the VTF equation. When $T < T_g$, T_f can be approximated by T_g for freshly prepared amorphous solid,[11] and Arrhenius-type temperature dependence of τ is observed at these temperatures. This similarity between crystallization rates and mean relaxation times suggests that the temperature dependence of $D(T)$ is much larger than that of $f(T)$ at temperatures $< T_g$, and that the crystallization rate of amorphous drugs may be estimated based on molecular mobility.

It would be of interest to expand the relationship between stability during storage and molecular mobility observed for pure amorphous drug systems to amorphous drug–excipient solid dispersion systems. Excipients have been reported to have an effect on the crystallization rates of some amorphous drugs.[9–17] Excipients stabilize amorphous drugs mainly due to (1) the anti-plasticizing effect of high T_g excipients (which results in an increase in the T_g, and therefore a decrease in the molecular mobility), and (2) specific interactions between the drug and the excipient. If the intensity of the specific interaction does not change to any great extent with the temperature, the crystallization rate of the drug in the solid dispersion can be expected to correlate with its molecular mobility.

In this study, the overall crystallization rates of nifedipine and phenobarbital were determined in the presence of poly(vinylpyrrolidone) (PVP) at temperature ranges above and below their T_gs, and were compared with the temperature dependence of their τ values, as obtained from the AGV equation.

EXPERIMENTAL

Materials

Crystalline nifedipine was purchased from Sigma (St. Louis, MO) and used as received. Crystalline phenobarbital was prepared from sodium phenobarbital (Wako Pure Chemical Industries, Osaka, Japan) according to a previously described method.[18]

Preparation of Nifedipine– and Phenobarbital–PVP Solid Dispersions

Nifedipine–PVP (9:1 w/w) and phenobarbital–PVP (95:5 w/w) solid dispersions were prepared by melting and rapidly cooling mixtures of each drug and PVP. Because the overall crystallization rate of phenobarbital was slower than that of nifedipine, lower PVP content was used for the phenobarbital solid dispersion to follow the crystallization kinetic under usual temperature conditions (25–80°C) within conventional experimental time periods. Crystalline nifedipine or phenobarbital was dissolved in methanol with PVP at w/w ratios of 9:1 and 95:9, respectively. The methanol was then evaporated off using a rotary evaporator under reduced pressure. The precipitate thus obtained was ground in a mortar, and then dried in a vacuum chamber at ~60°C for 1 day. A portion of the dried precipitate (~4 mg) was sealed into an aluminum sample pan with a pinhole in the lid, heated to ~190°C, cooled to −40°C at a cooling rate of −40°C/min, and reheated to room temperature in a differential scanning calorimeter (DSC; model 2920; TA Instrument, New Castle, DE).

To confirm that the prepared samples were amorphous, some of the prepared samples were opened before storage and examined by polarized light microscopy.

Determination of the Overall Crystallization Rates of Nifedipine and Phenobarbital in PVP Solid Dispersions

The sample pan containing nifedipine– or phenobarbital–PVP solid dispersion was transferred to

a vessel containing P_2O_5 and stored at a constant temperature (25–80°C). At appropriate intervals, samples were withdrawn, and the heat of crystallization (nifedipine) or the change in the heat capacity at T_g (phenobarbital) was measured. The heat of crystallization was measured at a heating rate of 20°C/min. Heat capacity at constant pressure (C_p) of the phenobarbital–PVP solid dispersion was also determined using a model 2920 modulated DSC equipped with refrigeration system (TA Instrument, New Castle, DE). The modulated temperature program used applied a modulation amplitude of ±0.5°C within 100 s, and had an underlying heating rate of 1°C/min.

Temperature and cell constant calibration of the instrument was carried out using indium, and the heat capacity was calibrated using sucrose.[2,19] High-performance liquid chromatography (HPLC) analysis of the stored samples showed no evidence of chemical degradation of nifedipine and phenobarbital.

Determination of the Enthalpy Relaxation Time

The solid dispersions prepared by the same method just described were stored at 25°C in vessels containing P_2O_5. At appropriate intervals, samples were withdrawn, and the relaxation enthalpy was measured at a heating rate of 20°C/min.

Heating Rate Dependence of T_g

The T_g values of the solid dispersions were measured at heating/cooling rates of 40, 20, 10, or 5°C/min. Samples of nifedipine– or phenobarbital–PVP precipitates (~4 mg) were heated to ~190°C and cooled to −40°C at rates of 40, 20, 10, or 5°C/min, then reheated at the same rates to 200°C. An aluminum cooling can filled with liquid nitrogen was used for cooling at 40 and 20°C/min. For measurements at heating/cooling rates of 10 and 5°C/min, the calorimeter was equipped with a refrigeration system.

Temperature calibration of the instrument was carried out at each heating rate using indium.

Calculation of the Relaxation Times of Amorphous Nifedipine and Phenobarbital According to the AGV Equation

The mean relaxation times (τ) of the nifedipine– and phenobarbital–PVP solid dispersions were calculated from the AGV equation (eq. 2; see Introduction).[1,2,8,20,21] The parameters D and T_0 in eq. 2 were calculated from the fragility, m, according to eqs. 3–5:

$$D = 2.303\,(m_{\min})^2/(m - m_{\min}) \tag{3}$$

$$m_{\min} = \log(\tau(T_g)/\tau_0) \cong \log(100/10^{-14}) = 16 \tag{4}$$

$$T_0 = T_g(1 - m_{\min}/m) \tag{5}$$

where $\tau(T_g)$ and τ_0 represent the relaxation times at T_g and at the upper temperature limit, which were assumed to be 100 and 10^{-14} s, respectively. The fragility, m, is defined as a temperature change in the relaxation time at T_g (eq. 6).

$$m = \frac{d(\log \tau)}{d(T_g/T)} \qquad T = T_g \tag{6}$$

Equation 6 can be approximated by eq. 7, which uses the activation energy (ΔH^*) for viscous flow.

$$m \cong \frac{\Delta H^*}{2.303RT_g} \tag{7}$$

The value of ΔH^* can be obtained from the scanning rate dependence of T_g as determined by DSC, as shown in eq. 8:

$$\frac{\Delta H^*}{R} = -\frac{d(\ln q)}{d(1/T_g)} \tag{8}$$

where R and q are the gas constant and heating rate, respectively. The fictive temperature, T_f, was assumed to be T_g in temperature ranges $<T_g$.

RESULTS AND DISCUSSION

Crystallization of Nifedipine and Phenobarbital in PVP Solid Dispersions

Typical thermograms of a nifedipine–PVP solid dispersion (9:1 w/w) stored at 70°C are shown in Figure 1. Glass transition was observed at ~50°C, and an exothermic peak attributable to the crystallization of amorphous nifedipine during the DSC heating process was observed at ~120°C with a freshly prepared solid dispersion. Two endothermic peaks due to melting of metastable and stable nifedipine crystal were observed at ~165 and 175°C, respectively, indicating that two polymorphs were formed from the amorphous phase. Relative areas of the melting peak for the two polymorphs did not significantly vary with storage time. Therefore, we assumed that the

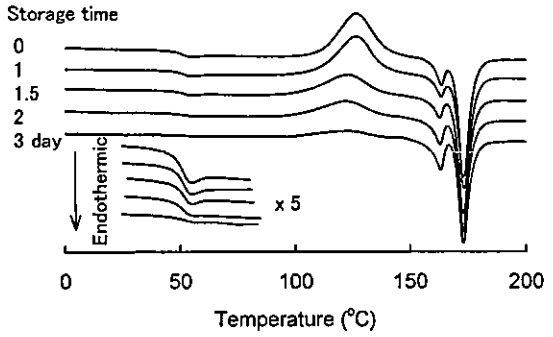

Figure 1. Typical thermograms of a nifedipine–PVP solid dispersion (9:1 w/w) stored at 70°C.

variation of relative amount of two polymorphs with storage time was negligible.

The area under the exothermic peak at ~120°C decreased as storage time increased, indicating that amorphous nifedipine crystallizes during storage at 70°C. We assumed that the area under the exothermic peak was proportional to the amount of amorphous nifedipine in the solid dispersion. The amount of amorphous nifedipine remaining [$R(t)$] was calculated using eq. 9:

$$R(t) = \Delta H_c(t)/\Delta H_c(0) \qquad (9)$$

where $\Delta H_c(0)$ and $\Delta H_c(t)$ represent the area under the exothermic peak prior to storage and after storage for time t, respectively.

The time profiles of the amount of amorphous nifedipine remaining in the solid dispersion are shown in Figure 2. It has been reported that the crystallization of nifedipine in a 2-hydroxypropyl-β-cyclodextrin matrix at temperatures $>T_g$ can be described by the Avrami–Erofeev equation[16]:

$$\{-\ln(1-\alpha)\}^{1/2} = kt \qquad (10)$$

The solid lines in Figure 2 represent the fit to this equation, as calculated by nonlinear regression, and indicate that the profiles of time versus of the amount of amorphous nifedipine remaining at temperatures of 50, 60, 70, and 80°C conform to the equation. It was difficult to determine an appropriate kinetic model from data obtained at lower temperatures because the decrease in the exothermic peak during storage for 2 years was too small. Therefore, we assumed that the same kinetic model could be applied to crystallization at lower temperatures. The time required for the amount of amorphous nifedipine to fall to 90% (t_{90}) was calculated from the rate constant obtained by nonlinear regression as a parameter of the crystallization rate.

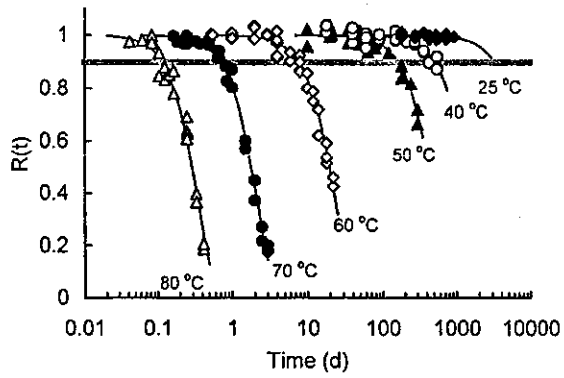

Figure 2. Time profiles of the amount of amorphous nifedipine remaining in nifedipine–PVP solid dispersions (9:1 w/w) stored at various temperatures.

Typical thermograms of a phenobarbital–PVP solid dispersion (95:9 w/w) are shown in Figure 3. A freshly prepared phenobarbital–PVP solid dispersion showed small endothermic peaks at ~160 and 175°C. In contrast, a broad exothermic peak appeared at ~130°C with the samples stored at 80°C. This peak initially increased with the storage time, but decreased once the storage time exceeded 6 h. The increase in the exothermic peak suggests that physical changes in solid dispersions may take place during storage at 80°C, and that these changes might induce the crystallization of phenobarbital during the DSC heating process. The decrease in the exothermic peak for samples stored for ≥6 h suggests that crystallization of phenobarbital may occur during storage at 80°C. Endothermic peaks at 160 and 170°C are attributable to the melting of phenobarbital crystals that arose from the amorphous phase during both storage at 80°C and the DSC heating process. These features make it difficult to estimate the amount of amorphous phenobarbital remaining in

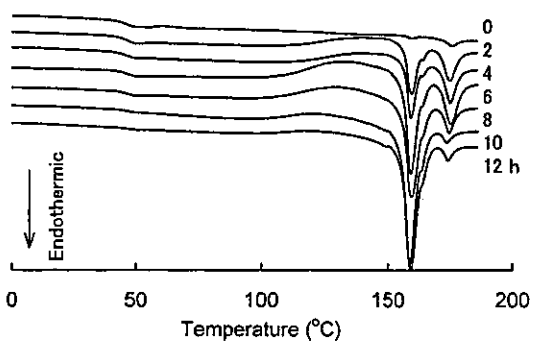

Figure 3. Typical thermograms of a phenobarbital–PVP solid dispersion (95:5 w/w) stored at 80°C.

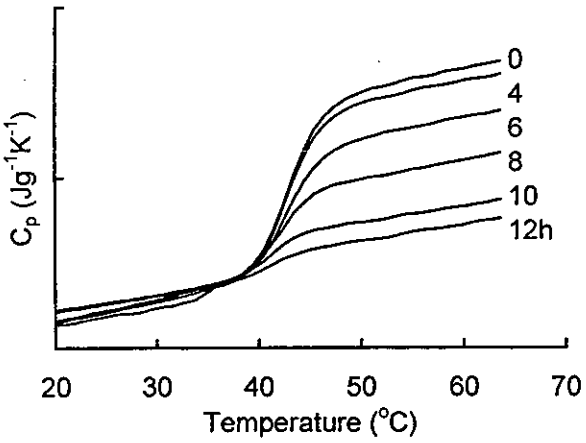

Figure 4. Changes in the heat capacity at T_g of a phenobarbital–PVP solid dispersion (95:5 w/w) stored at 80°C.

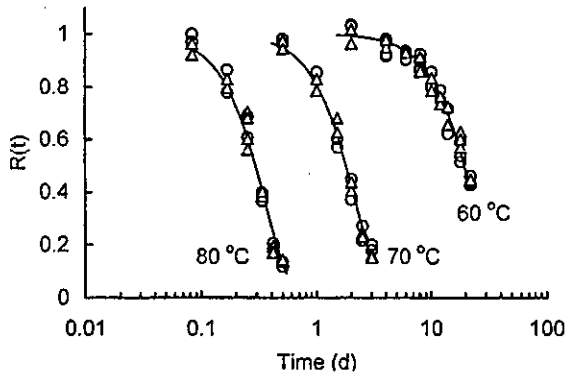

Figure 5. Time profiles of the amount of amorphous nifedipine remaining in nifedipine–PVP solid dispersion (9:1 w/w) stored at various temperatures. Key: (△) calculated from ΔC_p; (○) calculated from ΔH_c.

a solid dispersion from the exothermic peak at 130°C or the endothermic peaks at 160 and 170°C.

Changes in the heat capacity at T_g have been reported to be proportional to the amount of amorphous component in a mixture of an amorphous and a crystal drug.[22] As shown in Figure 4, changes in the heat capacity at T_g ($\Delta C_{p,Tg}$) for the phenobarbital–PVP solid dispersion decreased with the storage time, indicating that $\Delta C_{p,Tg}$ can be used as a measure of the amount of amorphous phenobarbital remaining.

$$R(t) = \Delta C_{p,Tg}(t)/\Delta C_{p,Tg}(0) \qquad (11)$$

To confirm the feasibility of using $\Delta C_{p,Tg}$ as a measure of the amount of amorphous drug remaining during the crystallization process, time profiles of $R(t)$ were calculated for the nifedipine–PVP solid dispersion from $\Delta C_{p,Tg}$ and ΔH_c data. The results are shown in Figure 5. The time profiles of $R(t)$ calculated from $\Delta C_{p,Tg}$ data were similar to those calculated from ΔH_c data, indicating that $\Delta C_{p,Tg}$ can be used as a measure of the amount of amorphous drug remaining.

The time profiles of $R(t)$ for phenobarbital–PVP solid dispersions stored at various temperatures are shown in Figure 6. The solid lines in the figure represent the fit to eq. 9 by nonlinear regression; t_{90} was calculated from the rate constant obtained by nonlinear regression.

The solid dispersions studied contained either 10 or 5% w/w of PVP. When crystallization of amorphous nifedipine or phenobarbital in the solid dispersions takes place, PVP is considered to separate from amorphous phase. This separation might affect the T_g of remaining amorphous phase. The T_g of the solid dispersions, however, did not show any tendency to increase or decrease during storage at temperatures above their T_g, as shown in Figures 1 and 4. Therefore, the effect of the PVP separated from amorphous phase on the T_g of the remaining amorphous phase can be considered negligible.

The temperature dependence of t_{90} of the solid dispersions is shown in Figure 7. The previously reported[23] t_{90} values for pure amorphous nifedipine and phenobarbital are also presented. When compared at the same storage temperatures, t_{90} values for these solid dispersions were ~100–1000 times longer than those for pure amorphous drugs.The T_g values (midpoint) for nifedipine– and phenobarbital–PVP solid dispersions were 51 and 46°C, respectively, at a heating rate of 20°C/min; these values were slightly higher than those

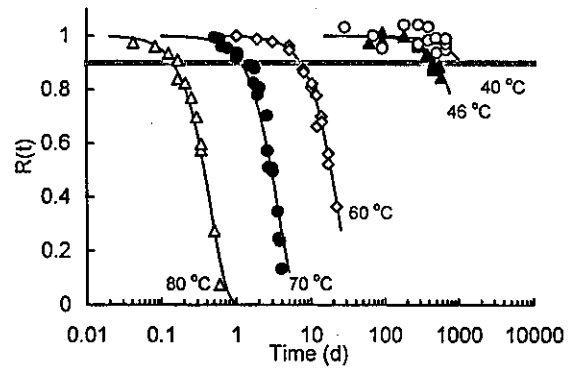

Figure 6. Time profiles of the amount of amorphous phenobarbital remaining in phenobarbital–PVP solid dispersion (95:5 w/w) stored at various temperatures.

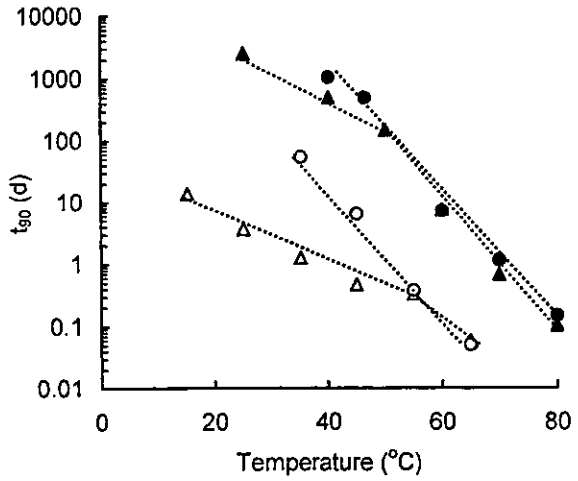

Figure 7. Temperature dependence of t_{90} for nifedipine–PVP (9:1 w/w) solid dispersions (▲), amorphous nifedipine (△), phenobarbital–PVP (95:5 w/w) solid dispersions (●), and amorphous phenobarbital (○).

for pure amorphous nifedipine (49°C) or phenobarbital (45°C).[23]

Stabilization by addition of a small amount of PVP has previously been reported for indomethacin–PVP and sucrose–PVP solid dispersions.[9–13] It has been reported that enthalpy relaxation of sucrose becomes slower when colyophilized with dextran, PVP, poly(vinylpyrrolidon-*co*-vinylacetate), or trehalose, even at a temperature at which the difference between T_g and storage temperature ($T_g - T$) is similar. This result indicates that the mobility of sucrose is reduced in the presence of the additives at temperature $<T_g$.[24]

Proportion of glass that has relaxed after storage at 25°C for nifedipine– and phenobarbital–PVP solid dispersions are shown in Figure 8. The previously reported[23] time profiles for the pure amorphous drugs are also shown. Enthalpy relaxation time (τ_e) of amorphous nifedipine, estimated according to the Kohlraush–Williams–Watts equation (eq. 12), increased from 1.2 to 18 days in the presence of 10% PVP, and the τ_e of amorphous phenobarbital increased from 1.0 to 3.7 days in the presence of 5% PVP.

$$\phi(t) = 1 - \frac{\Delta H_t}{\Delta H_\infty} = \exp\{-(t/\tau_e)^\beta\} \qquad (12)$$

where ΔH_t is the enthalpy recovered after storage for time t, β is a parameter that describes the distribution of relaxation time, and ΔH_∞ is the enthalpy change necessary for a glass to relax to a

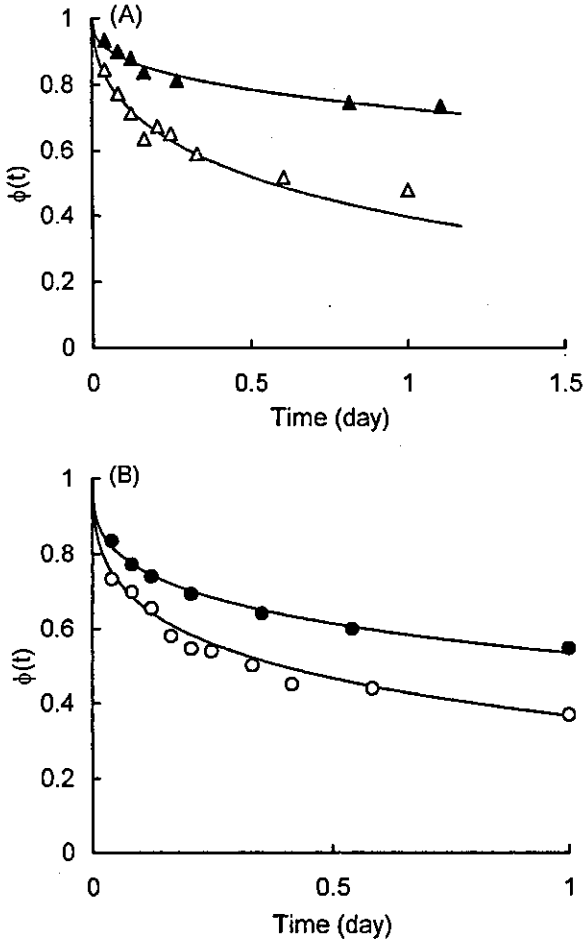

Figure 8. Proportion of glass that has relaxed for (A) nifedipine and (B) phenobarbital after storage at 25°C. Key: (△) nifedipine in the absence of PVP; (▲) nifedipine in the presence of PVP; (○) phenobarbital in the absence of PVP; and (●) phenobarbital in the presence of PVP. Solid lines were generated by fitting the data to the Kohlraush–Williams–Watts equation.

supercooled liquid. ΔH_∞ is calculated according to eq. 13[24]:

$$\Delta H_\infty = \Delta C_{p,Tg}(T_g - T) \qquad (13)$$

where ΔC_p is the change in the heat capacity at T_g, and T is storage temperature.

Although the increase in enthalpy relaxation time by addition of PVP was small compared with the increase in t_{90}, the stabilization of nifedipine and phenobarbital by a small amount of PVP may partly be attributable to the reduced molecular mobility.

Comparison of the Temperature Dependence of t_{90} and Relaxation Time

The crystallization rate, k, of an amorphous solid at temperature T depends on the rate of molecular diffusion across the nuclear–amorphous matrix interface [$D(T)$] and the nucleation free energy term [$f(T)$], according to eq. 1.[3–6] If the temperature dependence of $D(T)$ is much larger than that of $f(T)$, then t_{90} will be correlated with the mean relaxation time (τ) of the amorphous matrix as shown in eq. 14[1,7]:

$$t_{90}(T_g)/t_{90} \cong k/k(T_g) \cong D_T/D_{Tg} \cong (T/\eta)/[T_g/\eta(T_g)] \cong (T/\tau)/[T_g/\tau(T_g)] \quad (14)$$

where D_T and D_{Tg} are the diffusion coefficients at temperatures T and T_g, respectively.

The τ values for the solid dispersions were calculated according to the AGV equation, by the method previously reported by Zografi et al.[20,21] Because all degrees of freedom of motion contribute to the relaxation of amorphous materials, the mean relaxation time calculated according to the AGV equation has a distribution of relaxation mode that is reflected by the term β of the Kohlraush–Williams–Watts stretched exponential function. The heating rate dependence of the T_g values for the nifedipine–PVP solid dispersion is shown in Figure 9. The fragility of the solid dispersion was calculated from the slope of the line. The D and T_0 values of the AGV equation were calculated from the fragility obtained. The D value for the solid dispersion was estimated to be 15, which is similar to the value for pure amorphous nifedipine(14).[7] This similarity suggests that pure PVP may be as fragile as pure amorphous nifedipine.

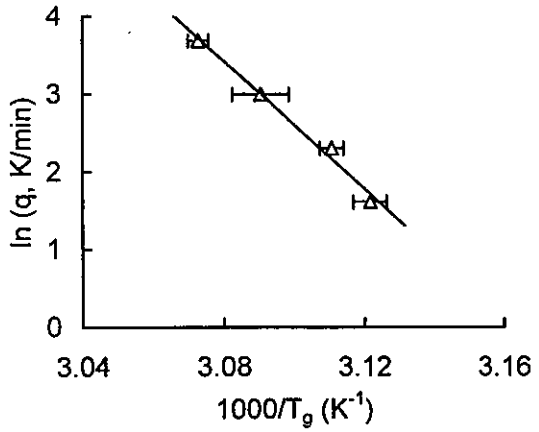

Figure 9. Heating rate (q) dependence of T_g for nifedipine–PVP (9:1 w/w) solid dispersions.

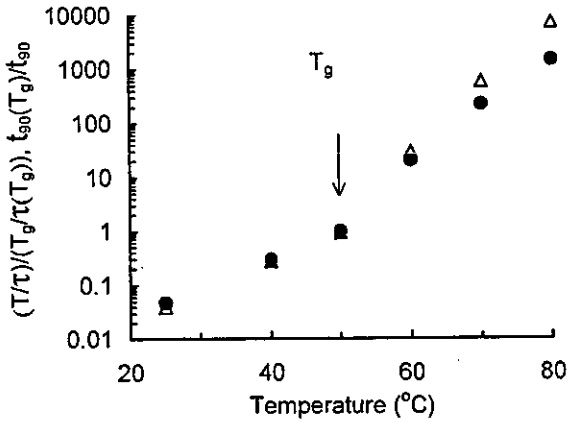

Figure 10. Temperature dependence of (△) $(T/\tau)/[T_g/\tau(T_g)]$ and (●) $t_{90}(T_g)/t_{90}$ for nifedipine–PVP (9:1 w/w) solid dispersions.

The parameters $(T/\tau)/[T_g/\tau(T_g)]$ and $t_{90}(T_g)/t_{90}$ are shown in Figure 10 as a function of temperature. The temperature dependence of $t_{90}(T_g)/t_{90}$ for the nifedipine–PVP solid dispersion seems coincident with that of $(T/\tau)/[T_g/\tau(T_g)]$ in the temperature range $<T_g$, within experimental error, albeit the temperature range studied was small. This result suggests that the temperature dependence of molecular motion [$D(T)$] is much larger than that of $f(T)$ at temperatures $<T_g$ in the presence of PVP. In other words, the free energy barrier for the molecular motion may be larger than that for the nuclei formation of amorphous nifedipine in the solid dispersion at temperatures $<T_g$, as reported for amorphous indomethacin crystallization.[25]

To predict the crystallization rate of amorphous drugs precisely, the temperature dependence of both the molecular mobility and the activation free energy of nuclei formation should be known. In practical purposes, however, the approximate t_{90} value of overall crystallization at temperatures $<T_g$ can be estimated from the information on the temperature dependence of molecular mobility and crystallization rate at temperatures around T_g.

REFERENCES

1. Guo Y, Byrn S, Zografi G. 2000. Physical characteristics and chemical degradation of amorphous

quinapril hydrochloride. J Pharm Sci 89:128–143.
2. Shamblin SL, Tang X, Chang L, Hancock BC, Pikal MJ. 1999. Characterization of the time scales of molecular motion in pharmaceutically important glasses. J Phys Chem B 103:4113–4121.
3. Hancock BC, Zografi G. 1997. Characteristics and significance of the amorphous state in pharmaceutical systems. J Pharm Sci 86:1–12.
4. Ngai KL, Magill JH, Plazek DJ. 2000. Flow, diffusion and crystallization of supercooled liquid: Revisited. J Chem Phys 112:1887–1892.
5. Saleki-Gerhardt A, Zografi G. 1994. Non-isothermal and isothermal crystallization of sucrose from the amorphous state. Pharm Res 11:1166–1173.
6. Rodriguez-Hornedo N, Murphy D. 1999. Significance of controlling crystallization mechanism and kinetics in pharmaceutical systems. J Pharm Sci 88:651–660.
7. Aso Y, Yoshioka S, Kojima S. 2001. Explanation of the crystallization rate of amorphous nifedipine and phenobarbital from their molecular mobility as measured by ^{13}C NMR relaxation time and the relaxation time obtained from the heating rate dependence of T_g. J Pharm Sci 89:128–143.
8. Hodge IM. 1987. Effects of annealing and prior history on enthalpy relaxation in glassy polymers. 6. Adam-Gibbs formulation of nonlinearity. Macromolecules 20:2897–2908.
9. Yoshioka M, Hancock BC, Zografi G. 1995. Inhibition of indomethacin crystallization in Poly(vinylpyrrolidone) coprecipitate. J Pharm Sci 84:983–986.
10. Matsumoto T, Zografi G. 1999. Physical properties of solid molecular dispersions of indomethacin with poly(vinylpyrrolidone) and poly(vinyl pyrrolidone-co-vinyl-acetate) in relation to indomethacin crystallization. Pharm Res 16:1722–1728.
11. Shamblin SL, Zografi G. 1999. The effect of absorbed water on the properties of amorphous mixtures containing sucrose. Pharm Res 16:1119–1124.
12. Zeng XM, Martin GP, Marriott C. 2000. Effects of molecular weight of polyvinylpyrrolidone on the glass transition temperature and crystallization of co-lyophilized sucrose. Int J Pharm 218:63–73.
13. Taylor LS, Zografi G. 1997. Spectroscopic characterization of interactions between PVP and indomethacin in amorphous molecular dispersions. Pharm Res 14:1691–1698.
14. Khougaz K, Clas S. 2000. Crystallization inhibition in solid dispersions of MK-0591 and poly(vinylpyrrolidone) polymer. J Pharm Sci 89:1325–1334.
15. Takeuchi H, Yasuji T, Yamamoto H, Kawashima Y. 2000. Temperature- and moisture-induced crystallization of amorphous lactose on composite particles with sodium alginate prepared by spray-drying. Pharm Dev Technol 5:355–363.
16. Hirayama F, Wang Z, Uekama K. 1994. Effect of 2-hydroxy-β-cyclodextrin on crystllization and polymorphic transition of nifedipine in solid state. Pharm Res 11:1766–1770.
17. Uekama K, Ikegami K, Wang Z, Horiuchi Y, Hirayama F. 1992. Inhibitory effect of 2-hydroxypropyl-β-cyclodextrin on crystal-growth of nifedipine during storage: superior dissolution and oral bioavailability compared with polyvinylpyrrolidone K-30. J Pharm Pharmacol 44:73–78.
18. Kato Y, Watanabe F. 1978. Relationship between polymorphism and bioavailability of phenobarbital. Yakugaku Zasshi 98:639–648.
19. Putnam RL, Boerio-Goates J. 1993. Heat-capacity measurements and thermodynamic functions of crystalline sucrose at temperatures from 5 K to 342 K. Revised values for $\Delta_f G^\circ_m$ (sucrose, cr, 298.15 K), $\Delta_f G^\circ_m$ (sucrose, aq, 298.15 K), S°_m (sucrose. aq, 298.15 K); and $\Delta_r G^\circ_m$ (298.15 K) for hydrolysis of aqueous sucrose. J Chem Thermodyn 25:607–613.
20. Andronis V, Zografi G. 1998. The molecular mobility of supercooled amorphous indomethacin as a function of temperature and relative humidity. Pharm Res 15:835–842.
21. Tong P, Zografi G. 1999. Solid-state characteristics of amorphous sodium indomethacin relative to its free acid. Pharm Res 16:1186–1192.
22. Guinot S, Leveiller F. 1999. The use of MTDSC to assess the amorphous phase content of micronised drug substance. Int J Pharm 192:63–75.
23. Aso Y, Yoshioka S, Kojima S. 2000. Relationship between the crystallization rates of amorphous nifedipine, phenobarbital, and flopropione, and their molecular mobility as measured by their enthalpy relaxation and ^1H NMR relaxation times. J Pharm Sci 89:408–416.
24. Shamblin SL, Zografi G. 1998. Enthalpy relaxation in binary amorphous miztures containing sucrose. Pharm Res 15:1828–1834.
25. Andronis V, Zografi G. 2000. Crystal nucleation and growth of indomethacin polymorphs from the amorphous state. J Non-cryst Solids 271:236–248.

Application of Sterylglucoside-Containing Particles for Drug Delivery

Yoshie Maitani[1,*], Koji Nakamura[2] and Kumi Kawano[1]

[1]*Institute of Medicinal Chemistry and* [2]*Department of Pharmaceutics, Hoshi University, Ebara 2-4-41, Shinagawa-ku, Tokyo, Japan 142-8501*

Abstract: Recent advances in biotechnology have promoted biomolecular targeting of drugs, peptides and genes in the treatment and management of major diseases and infections. Therapeutic development of drugs and delivery systems may have various objectives: Systemic drugs require optimal delivery and uptake at target sites; peptide drugs require alternative routes of administration, such as nasal or intestinal absorption; gene medicines need to be delivered efficiently, safely and selectively to diseased areas. The propensity of ligand-modified liposomes to carry drugs and genes to desirable sites has been extensively examined and current reports show considerable progress in this field. Sterylglucoside (SG) is a novel absorption-enhancer of peptide drugs across nasal and intestinal mucosae. Physico-chemical properties and biodistribution of liposomes incorporating SG were studied and compared against the profiles of aglycon and sitosterol derivatives of SG. It was shown that SG particles aided colon drug delivery and increased bioavailability of peptide drugs after nasal and intestinal administration. In addition, they were able to enhance anticancer effects in liver cancer chemotherapy. Biological fate and interaction of SG with hepatocytes support the novel proposition of liver-targeting SG-liposomes.

Key Words: sterylglucoside; absorption enhancer; insulin; nasal absorption; nanoparticle; colon drug delivery; liver-targeting; anti-tumour drug.

INTRODUCTION

Recent advances in biotechnology have promoted molecular targeting of drugs, peptides and genes in the treatment and management of major diseases and infections. However, the administration routes and dosage forms of modern therapeutic drug delivery systems (DDS) have not evolved to complement and further such progress. Development of therapeutic DDS often aim for a variety of different goals. For example, peptide drugs are better suited to oral or nasal administration rather than systemic injection, and systemic drugs would benefit from optimal delivery and uptake at target sites.

Progress in biotechnology has led to the development of processes and the establishment of facilities for producing large quantities of peptide-based pharmaceuticals on an economical scale. This has made the therapeutic use of many peptide and protein pharmaceuticals feasible and practical. Since peptides and proteins are high molecular-weight macromolecules, they do not easily permeate into human intestinal mucosae. Oral or nasal administration exposes them to proteolytic enzymes in the gastrointestinal (GI) tract or nasal cavity, considerably reducing systemic bioavailability and efficacy. Penetration enhancers, such as bile salts and surfactants, may be co-administered to improve absorption. However, most types are harmful to intestinal and nasal epithelia. The search for safe and effective absorption enhancers is an important and on-going task.

Cancer is the highest cause of death all over the world. Conventional anticancer drugs are predominantly cytotoxic; indiscriminate destruction of diseased and normal cells limits their therapeutic dose and routes of administration. The ability to target such drugs would be desirable since it would increase efficacy and decrease unwanted side-effects. Drug-targeting strategies may be classified as either "prodrug" or "carrier-mediated" systems. Pro-drugs are drug-related chemical precursors that become converted into their active forms at the site of action. Carrier-mediated systems involve either covalent or non-covalent association of drug molecules with a targeting moiety, which facilitates transport of drugs into target cells. Particulate systems, such as nanoparticles, nanospheres, emulsions, liposomes and mixed micelles, have been recently investigated as potential carrier systems for delivery and targeting of drugs to specific sites in the body. Modification of particles with specific ligands, such as antibodies, glycoconjugates, or peptides, enables active-targeting of tumour tissues.

The majority of absorption enhancers exhibit water-soluble properties, but a few can also be oil-soluble, such as fatty acids. Sterylglucoside (SG) is a soybean extract and comprises of four analogues (Fig. 1), primarily β-sitosterol β-D-glucoside (Sit-G), which exhibits slight solubility in water and in oil. Particulate SG exhibited the novel capability of promoting transport of peptide drugs through intestinal and nasal mucosae, as well as targeted delivery to hepatic tissues. The following topics will be discussed in detail:

1. Physicochemical properties of Sit-G nanoparticles (Sit-G NP) and liposomes containing SG (SG-liposomes), as compared with its aglycon.
2. Absorption enhancer: the efficacy of Sit-G NP and SG-liposomes in nasal and intestinal absorption of insulin and the mechanism of enhancer action.

*Address for correspondence to this author at the Institute of Medicinal Chemistry, Hoshi University, Ebara 2-4-41, Shinagawa-ku, Tokyo, 142-8501 Japan; Tel/Fax: 81-3-5498-5048; E-mail: yoshie@hoshi.ac.jp

1389-2010/05 $50.00+.00 © 2005 Bentham Science Publishers Ltd.